PPP carrier phase residual stacking for turbulence investigations

Franziska Kube and Steffen Schön
Institut für Erdmessung | Leibniz Universität Hannover

Leibniz Universität Hannover

Introduction

Microwave space-geodetic observations such as Global Navigation Satellite Systems (GNSS) or Very Long Baseline Interferometry (VLBI) are delayed in the neutral atmosphere. In order to improve the quality of these techniques for precise applications like reference frame realisation, we need to get more knowledge about the temporal and spatial refractivity variations in the neutrosphere. In addition to the annually to hourly long periodic variations, which can be considered within the adjustment process, micro-scale meteorological phenomena in the range of minutes to sub-second affect space-geodetic observations as well. Thus, induced phase fluctuations of wavefronts passing through the turbulent medium form a significant error source for electromagnetic wave propagation on the one hand side. On the other side, they reveal information about the turbulent media through which the signal has travelled and thus can be used to enhance the modelling of neutrospheric refraction.
In order to identify high-frequency atmospheric effects, we analysed 1Hz high-rate GPS observations from the continuous operating GNSS station at the Geodetic Observatory Wettzell and derived post-fit carrier phase residuals for several days with a Kalman-Filter based Precise Point Positioning (PPP) approach. Since undifferenced carrier phase observations contain a superposition of several effects, the computed power-law behaviour of the residuals might not follow the theoretically predicted stochastical behaviour for refractivity fluctuations. Hence, first the influence of multipath was identified. A residual stacking was performed, and the reduced residuals were analysed with regard to turbulenct characteristics.

PPP analysis and residual stacking

A daily PPP analysis was performed for the station *WTZR* for 17 consecutive days in 2011 with the IfE-MATLAB toolbox. We choosed this time and station in order to study the variability of water vapour in the atmosphere and the resulting refraction effects with two techniques in the radio frequency domain (GPS and VLBI) in parallel. We used a Kalman Filter approach (see Tab. 1 for settings) to generate L3 1 Hz GPS carrier phase residuals.

Tab. 1: PPP analysis settings.

Processing time interval	DoY 257-273 2011 & Sundays DoY 072:7:359 2011
Elevation cut-off angle	5 $^\circ$
observation weighting	elevation dependent $sin^2(E)$
Sampling rate	1 s
EOP/Satellite orbits & -clocks	CODE final, CODE.CLK (5 s), linearly interpolated to 1 s [Bock et al., 2009]
Satellite antenna	absolute antenna model from IGS08.atx
Receiver antenna	individual absolute calibration
Troposphere a priori model	Saastamoinen Model, mapped with VMF1
Troposphere modelling	random walk with process noise of 15 $^{mm}/\sqrt{h}$
Static coordinates modelling	Random constant
Carrier phase ambiguities modelling	Random constant
Receiver clock model	2-state-model [van Dierendonck et al., 1984], [Weinbach and Schön, 2011]

The L3 phase residuals show variations of about ± 80 mm and an elevation dependent behaviour, see Fig. 2(a) exemplary for one day and selected satellites. Apart from turbulence effects, the phase residuals contain superpositions of several effects, such as residual receiver and satellite clock variations, receiver noise, and multipath. In order to reduce their impact and to study the turbulence, we applied a receiver clock modelling [Weinbach and Schön, 2011], used high-rate satellite clock corrections [Bock et al., 2009] and generated a statistically robust multipath stacking map [Fuhrmann et al., 2015]. Congruent cell with an azimuth resolution of 2 $^\circ$ at the local horizon and elevation resolution of 1 $^\circ$ were computed. In addition to the days during the VLBI CONT11 campaign, we computed PPP L3 phase residuals for other 39 days in 2011. Overall 56 days of PPP analysis yield 43.947.448 L3 phase residuals, with 163.6140 outlier (0, 4%) and 273 residuals (0, 0006%) in cells with less than 15 residuals. As expected, the multipath stacking map shows smaller variations and standard deviations at lower elevation and vice versa, see Fig. 1(a) and 1(b). An indicator for multipath might the higher standard deviation in a sector between 150 $^\circ$ and 190 $^\circ$ at 45 $^\circ$ elevation.
After removing the computed mean stacked values from the original residuals, variations, especially at higher elevations are removed and the histogramm shows less values exceeding ± 15 mm, see Fig. 2(b) and 2(c).

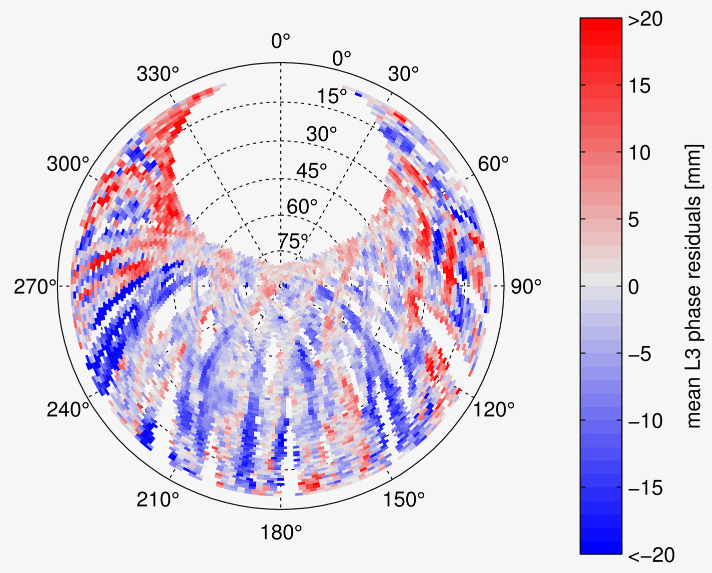

(a) WTZR mean stacked L3 phase residuals for 56 days in 2011.

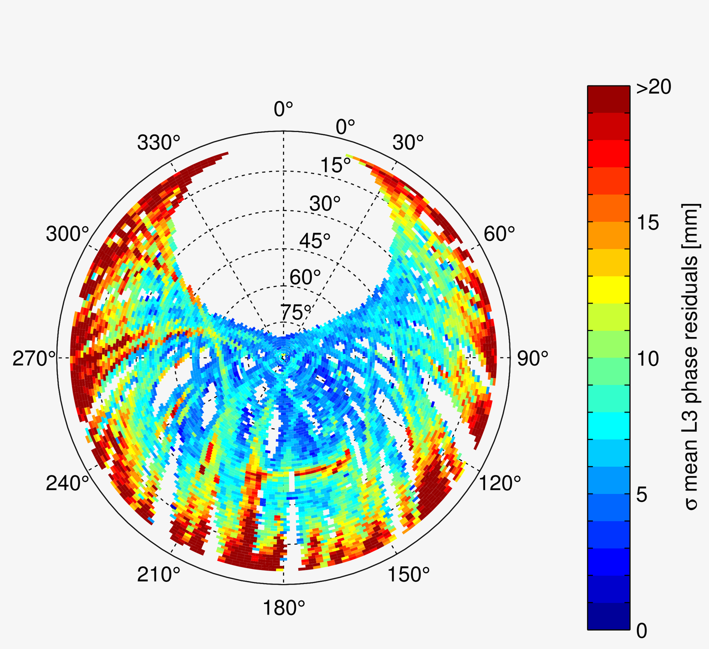

(b) WTZR standard deviation of mean stacked L3 phase residuals.

Fig. 1: PPP L3 phase residuals stacking map with corresponding standard deviation.

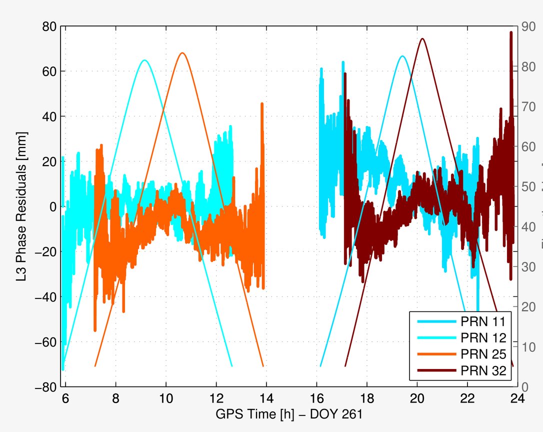

(a) WTZR DoY 261 original L3 phase residuals.

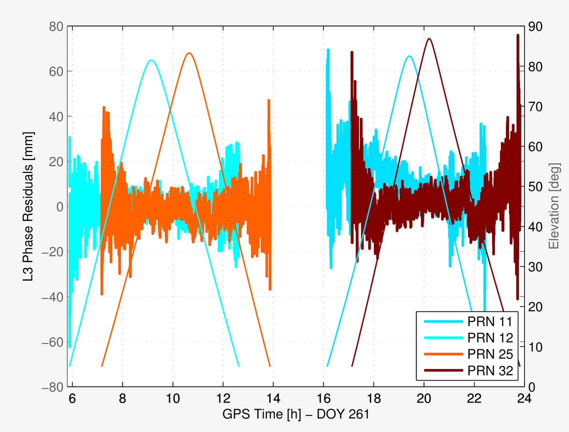

(b) WTZR DoY 261 reduced L3 phase residuals.

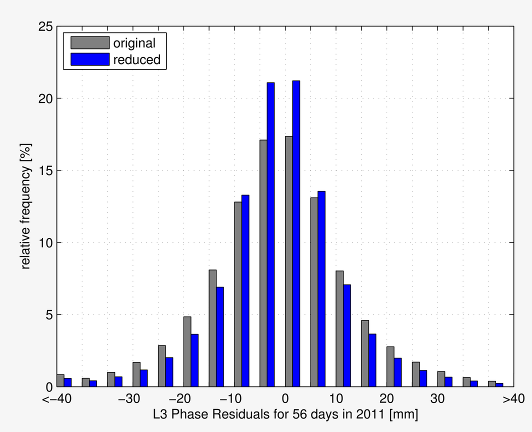

(c) WTZR DoY histogram of original and reduced L3 phase residuals for 56 days in 2011.

Fig. 2: PPP L3 phase residuals before and after multipath stacking and their distribution.

Stochastic tools for turbulence investigations

High-frequency turbulence effects can be best described stochastically. Following the widely accepted Kolmogorov turbulence model, refractivity fluctuations can be characterised by specific power-law processes. In order to identify these fluctuations in the resulting phase residuals, dedicated analysis tools are applied such as temporal structure functions (Fig. 3(a) and 3(d)), power spectrum (Fig. 3(b) and 3(e)) or the Allan variance (Fig. 3(c) and 3(f)).

The prevailing turbulent regime is then characterized by the shape of the structure function yielding typical slopes in a log-log-plot ranging from $^5/_3$ to $^2/_3$ for small separations τ and finally reaching 0 for large τ [Wheelon, 2001]. In addition, the slope of power spectrum or Allan variance can be used as indicator for turbulence processes [Thompson et al., 2001] (see Tab. 2).

Since undifferenced carrier phase residuals contain a superposition of several unmodelled effects, the computed slopes from the original residuals will not clearly show the theoretical values. Thought, residual stacking and removing the stacked values will reduce the residual multipath effect, we expected to approximate the slope values from literature and thus identify turbulence effects in the reduced phase residuals.

Tab. 2: Power law relations for turbulence.

Quantity	Exponent: 3D turbulence (very small τ)	Exponent: 2D turbulence (small τ)
(Temporal) structure function	$^5/_3$	$^2/_3$
phase spectrum	$-^8/_3$	$-^5/_3$
Allan variance	$-^1/_3$	$-^4/_3$

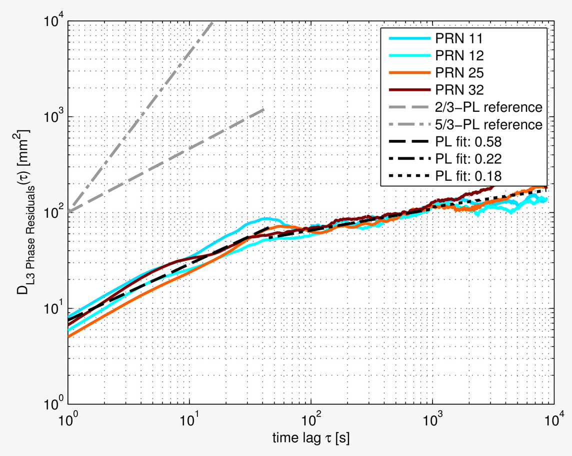

(a) temporal structure function of original L3 phase residuals

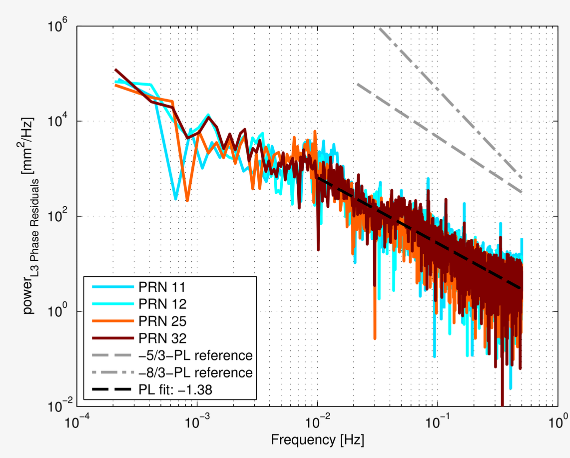

(b) power spectrum of original L3 phase residuals.

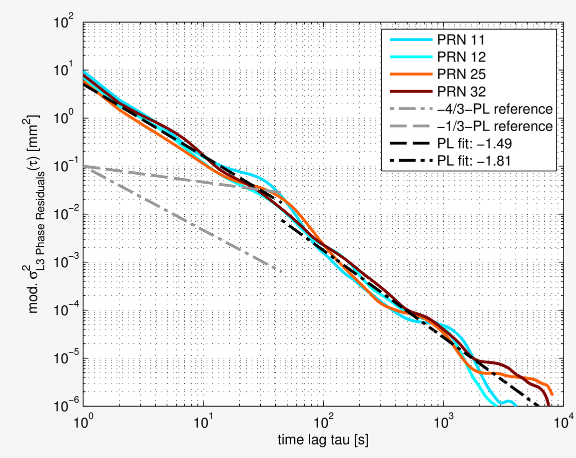

(c) modified Allan Variance of original L3 phase residuals.

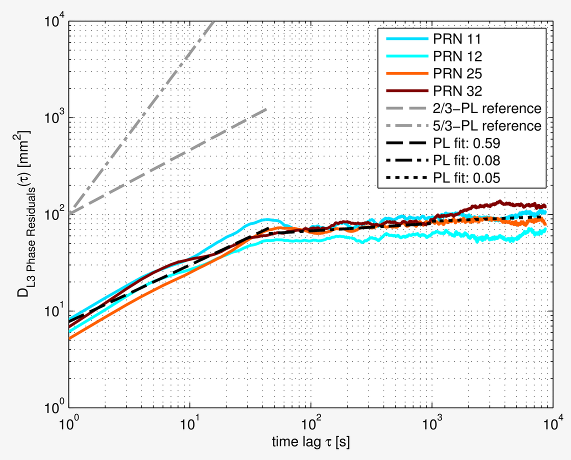

(d) temporal structure function of reduced L3 phase residuals.

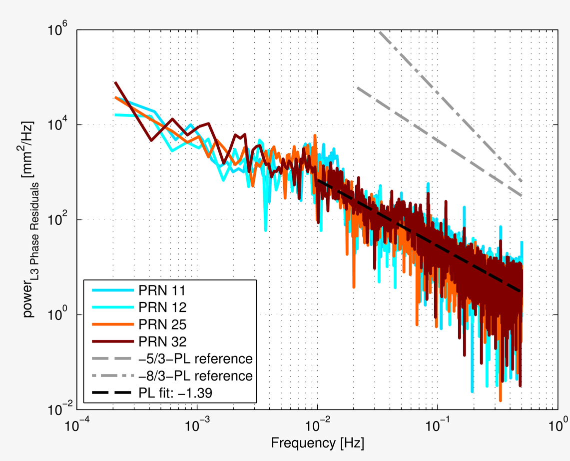

(e) power spectrum of reduced L3 phase residuals.

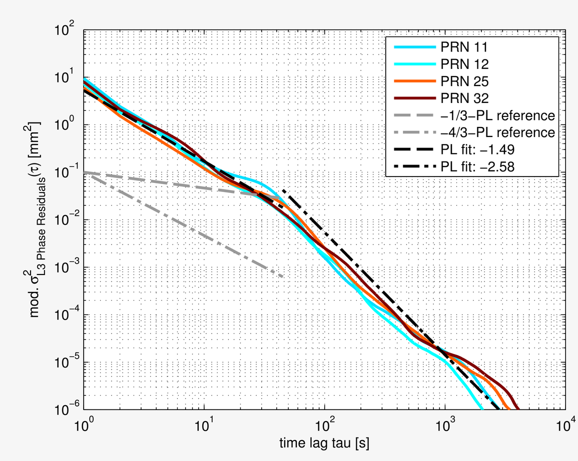

(f) modified Allan Variance of reduced L3 phase residuals.

Fig. 3: Statistics of computed PPP L3 phase residuals and reduced residuals.

Conclusions and Outlook

- We performed 56 days of daily 1 Hz PPP analysis in order to generate a large number of residuals for statistically robust multipath stacking. The mean values were reduced from the original residuals and the resulting reduced residuals were analysed with regard to turbulent effects.
- The theoritical values for slopes in log-log plot of temporal structure function, power spectrum and Allan variance cannot be observed in original and reduced residuals for very small τ. For time lags up to $\sim$45 s (small τ), the slopes nearly reaches the expected values. There is a slight change resulting from residual stacking and reduction in the computed power-law behaviour for these time lags. For longer time lags, the influence is most significant.
- For time lags up to $\sim$45 s a slope of $\sim {}^2/_3$ can be observed in the temporal structure function. For larger time lags, the slope nearly reaches 0 in the reduced residuals. Hence long periodic effects are reduced by the performed stacking and reduction, see Fig. 3(a) and 3(d).
- In the power spectrum of phase residuals a slope of $\sim -^5/_3$ is noticeable for periods up to $\sim$100 s. A peak in the spectrum appears at $\sim$20 s and $\sim$100 s. For periods up to $\sim$1000 s the slopes nearly reaches 0 and then changes again, see Fig. 3(b) and 3(e).
- The modified Allan variance shows a continuous $\sim -^4/_3$ behaviour for periods up to $\sim$45 s. For larger periods it is changing to a more steep negative slope of ~ -2 and ~ -2.6 for the reduced residuals respectively, see Fig. 3(c) and 3(f).
- Further investigations will concentrate on Kalman filter settings and the simulation of turbulence effects in order to analyse in which step of geodetic data processing atmospheric turbulence can be observed.

References

[Bock et al., 2009] High-rate GPS clock corrections from CODE: support of 1 Hz applications. *Journal of Geodesy*, 83:1083–1094.

[Fuhrmann et al., 2015] Generating statistically robust multipath stacking maps using congruent cells. *GPS Solutions*, 19(1):83–92.

[Thompson et al., 2001] *Interferometry and Synthesis in Radio Astronomy*. John Wiley & Sons, 2nd edition.

[van Dierendonck et al., 1984] Relationship between Allan Variances and Kalman Filter Parameters. In *Proccedings of the 16th Annual PTTI Meeting 1984*.

[Weinbach and Schön, 2011] GNSS receiver clock modeling when using high-precision oscillators and its impact on PPP. *Advances in Space Research*, 47(2):229–238.

[Wheelon, 2001] *Electromagnetic Scintillation I: Geometrical Optics*. Cambridge University Press.

Acknowledgement

The authors thank the German Research Foundation (DFG) for its financial support (SCHO 1314/3-1) and the BKG for the GPS data at Wettzell. We further acknowledge the International GNSS Service (IGS) and the Center for Orbit Determination in Europe (CODE) for its products.

Created with LaTeX beamerposter, IUGG Poster #G01p-245

Institut für Erdmessung
Schneiderberg 50
D-30167 Hannover

IUGG General Assembly 2015
Prague, Czech Republic
June 22nd-July 2nd 2015

Franziska Kube
Steffen Schön
www.ife.uni-hannover.de
{kube, schoen}@ife.uni-hannover.de